The CLAS12 Micromegas Vertex Tracker

A. Acker, D. Attié, S. Aune, J. Ball, P. Baron, Q. Bertrand, D. Besin, T. Bey, F. Bossù, R. Boudouin, et al.

Version of Record: https://www.sciencedirect.com/science/article/pii/S0168900220300280
Manuscript_85c6fe7341b4b9d24b069b77ae461982

The CLAS12 Micromegas Vertex Tracker

A. Acker, D. Attié, S. Aune, J. Ball, P. Baron, Q. Bertrand, D. Besin, T. Bey, F. Bossù, R. Boudouin, M. Boyer, G. Christiaens, P. Contrepois, M. Defurne, E. Delagnes, M. Garçon, F. Georges, J. Giraud, R. Granelli, N. Grouas, C. Lahonde-Hamdoun, T. Lerch, I. Mandjavidze, O. Meunier, Y. Moudden, S. Procureur, M. Riallot, F. Sabatié, M. Vandenbroucke, E. Virique

IRFU, CEA, Université Paris-Saclay, 91191, Gif-sur-Yvette, France

Abstract

The Micromegas Vertex Tracker was designed to improve upon the tracking capabilities of the baseline design of the CLAS12 spectrometer in Hall B at Jefferson Laboratory. A Barrel Micromegas Tracker made with six concentric cylinders, each made of three 120°-sector tiles, surrounds the Silicon Vertex Tracker, and a Forward Micromegas Tracker composed of 6 disks is placed 30 cm downstream of the liquid-hydrogen target. Both trackers sit in a 5 T solenoid magnetic field. All Micromegas elements are based on resistive technology to withstand luminosities up to 10^{35} $\mathrm{cm}^{-2}\mathrm{s}^{-1}$, as well as on bulk technology to enforce gain uniformity and mechanical robustness. Due to the high magnetic field, dedicated electronics have been designed and displaced ∼2 m away from the detectors. The electronics readout is based on the DREAM ASICs that allow sustained operation up to 20 kHz trigger rate at the maximum luminosity.

1. Introduction

The baseline design of the Hall B CEBAF Large Acceptance Spectrometer for use at the 12 GeV Jefferson Laboratory (JLab) facility (CLAS12) [1] includes two tracking detector systems. A Silicon Vertex Tracker (SVT) [2] consists of a polyhedral arrangement around the target and resides in a 5 T solenoid magnetic field to detect particles emitted between 35° and 125° with respect to the beam direction. The forward tracking system consists of drift chambers [3] placed before, within, and after a toroidal magnetic field and covers the polar angle interval between 5° and 35°.

In 2010, a proposal submitted by the IRFU group at CEA-Saclay for an upgrade of the baseline CLAS12 design was accepted by JLab management. The upgrade of the central tracker consisted of replacing the fourth layer of the SVT baseline design with 6 layers of cylindrical Micromegas detectors, called the Barrel Micromegas Tracker (BMT). In addition, a Forward Micromegas Tracker (FMT) made of 6 Micromegas disks was placed ∼30 cm downstream of the target to supplement the forward tracking system with the drift chambers. The FMT and BMT form the Micromegas Vertex Tracker (MVT). Simulations showed that the addition of the Micromegas detectors improved the vertex and polar angle resolutions both in the central and in the forward tracking systems compared to the baseline design [4, 5].

Together, the SVT and the BMT form the Central Vertex Tracker (CVT). The CVT is surrounded by two scintillator-based detectors called the Central Time-Of-Flight (CTOF) [6] and the Central Neutron Detector (CND) [7] that provide particle identification information.

2. System Description

2.1. Micromegas Detectors

Micromegas detectors are micro-pattern gaseous detectors [8]. A schematic representation of a typical Micromegas detector is shown in Fig. 1. In the few-millimeter-wide conversion gap with an electric field of a few kV/cm, free electrons produced by the ionization of gas molecules by charged particles drift toward the micro-mesh and enter the amplification gap. In the amplification gap, the electric field reaches several hundreds of kV/cm, accelerating the electrons arriving from the conversion gap

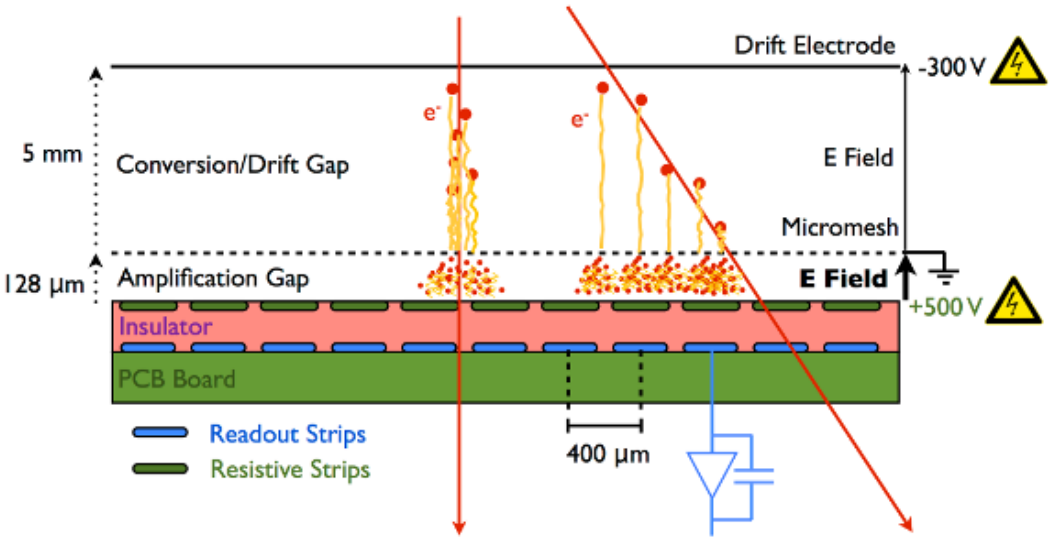

Figure 1: Schematic view of a resistive Micromegas detector.

and making them ionize the gas, consequently creating an electromagnetic shower. The signal is then collected by the readout strips.

The MVT must sustain a high particle flux, which may induce sparks between the micromesh and the strips in its nominal running conditions. In order to quench these sparks and their associated temporary high voltages (HV) drops that "blind" the detector, all MVT detectors are based on the resistive technology. As depicted in Fig. 1, resistive strips and a thin layer of insulator are deposited on top of the readout strips [9]. The signals are transferred from the resistive to the readout strips by capacitive coupling. Finally, the resistive technology allows for higher gains to be reached compared to regular detectors due to a lower probability of sparks in the amplification region. Consequently the resistive technology allows for higher signal to background ratios. In this configuration the mesh is grounded and the high voltage for amplification is positive on the resistive strips.

2.2. General

The Barrel Micromegas Tracker consists of six layers of cylindrical detectors, three with strips along the beam axis (Z strips) that provide information about the azimuthal angle of the particle and three with circular strips (C strips) perpendicular to the beam axis that significantly improve the polar angle determination with respect to that extracted from the SVT information alone. The strip orientation, the pitch, and the radial distance from the center are listed in Table 1. Each layer is made of three curved detectors covering 115° each. A total of 18 curved detectors is assembled on a carbon structure to complete the BMT. In addition to the resistive technology, these detectors make use of the bulk technology, meaning that the micromesh is embedded with the pillars on top of the resistive strips [10]. The bulk technology enforces a uniform distance between the micromesh and the strips, consequently maintaining a uniform gain over the detector surface, despite the mechanical stress induced by the curvature of the tile.

Radius (mm)	Pitch (μm)	Strip orientation
146.146	330 - 860	C
161.146	487	Z
176.146	536	Z
191.146	340 - 770	C
206.146	529	Z
221.146	330 - 670	C

Table 1: Radius, pitch, and strip orientation of the different BMT layers.

The Forward Micromegas Tracker consists of six flat Micromegas disks stacked together. The disks are all identical and assembled with a 60° rotation with respect to one another, giving 3 angles of strips (0°, 60°, and 120°). The FMT is attached to the downstream end flange of the BMT. Figure 2 dis-

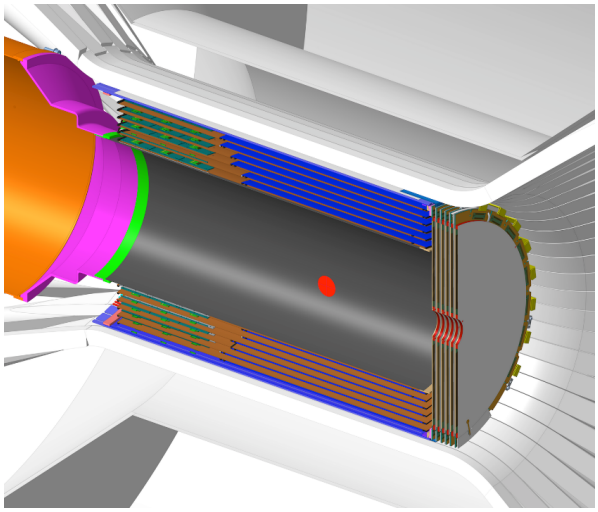

Figure 2: Cut view showing the 6 different layers of the BMT and the 6 identical FMT disks. The detectors are inserted close to the Central Time-of-Flight, itself in the 5 T solenoid magnet. The SVT is inside the MVT and is not displayed in this view where the beam enters from the left. The red dot indicates the nominal target position.

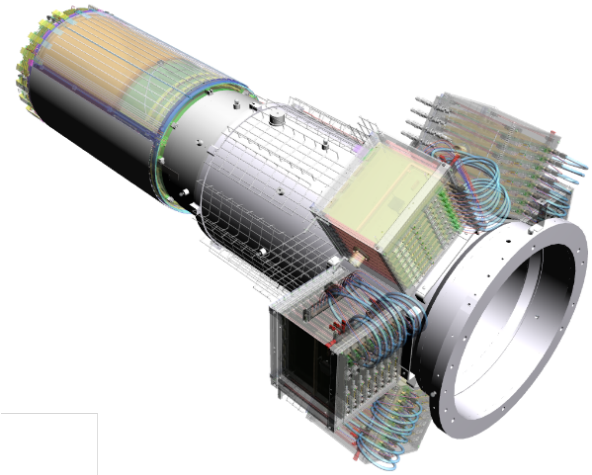

Figure 3: Support tube with electronics rack and MVT detectors. The beam enters from the right.

plays a cut view of both the BMT and FMT inside the CLAS12 solenoid magnet.

A separate CLAS12 subsystem called the Forward Tagger (FT) that is positioned just upstream of the torus magnet and covers polar angles from 2° to 5°, also includes a set of Micromegas trackers. The FT is equipped with four Micromegas disks arranged in two pairs, called the FT Tracker (FT-Trk), which shares most of its design with the FMT. A detailed description can be found in Ref. [11].

2.3. Mechanical Structure

In order to support the Micromegas Vertex Tracker in the magnet, a stainless-steel tube with the BMT and the FMT at its downstream end is attached to the flange of the SVT support tube, as shown in Fig. 3. This tube also holds 6 crates containing the 48 readout Front-End Unit (FEU) boards for the Micromegas detectors, as well as the service distributions for the gas, environmental sensors, and high-voltage distribution. The connection between the detectors and readout FEUs is done using assembled micro-coaxial cables that allow the signals to be read out from the upstream electronics crates. Each FEU is connected to a Back-End Unit with an optical fiber. The patch panels for the gas and the high voltage cables are located on the 6 crates.

The mechanical structure of the BMT is made of a thin (1 mm) carbon cylinder with a glued PEEK flange downstream, and a glued stainless-steel flange upstream, as shown in Fig. 4. Since the main purpose of the barrel is to reconstruct protons with momentum as low as 300 MeV, the material budget must be as small as possible in order to reduce multiple scattering and energy loss. The stainless steel used for the tube and flanges is made of 904L (non-magnetic steel). The BMT structure is completed by an outer thin carbon-fiber cylinder that protects the BMT tiles during maintenance operations. The detector alignment is performed using particle tracks taken during zero magnetic field data taken either with cosmic rays (as described in Section 4.2) or with the electron beam.

2.4. Barrel Micromegas Tracker (BMT)

The Barrel detector tiles are made of a thin printed circuit board (PCB) (0.2 mm) transformed into Micromegas with the bulk process. Up to 16 MEC8 connectors are welded on the upstream end of the tile. The PCB is curved on a custom mandrel tool with the desired radius. The cylindrical shape is then maintained by gluing two carbon fiber arcs at each end of the active zone and two aluminum arcs on the MEC8 connector side. The thickness of the carbon and aluminum structure arcs (3 mm) was chosen to match the design drift gap of the detectors. A Kapton foil (0.25 mm) with metallic coating is then glued on top of the carbon-

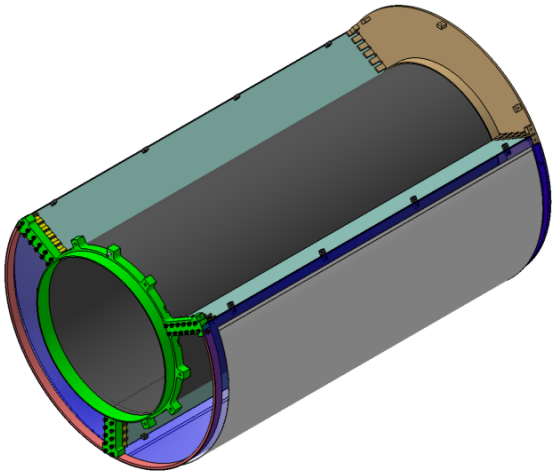

Figure 4: BMT mechanical structure (shown with one sector open) that houses 6 curved detectors.

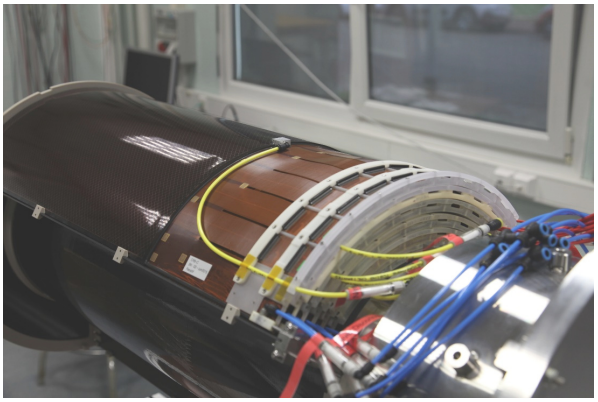

Figure 5: Photograph of a full stack of 6 BMT layers. The two aluminum arcs are visible on top of the connectors. The blue and yellow plastic tubes are part of the gas plumbing.

aluminum structure to seal the detector and serves as the drift electrode of the detector. A curved 3D-printed plastic mechanical bracket is attached above the connectors to provide rigidity for the connection of the signal cables. The high voltage connections and the associated protection circuit are hosted inside 4 cm $\times$ 8 cm metallic boxes on the upstream side of the PCB, out of the active area. Gas is introduced in the middle of the connector side and flushed out on the edges of the connector side through the hollow carbon-aluminum mechanical structure. The leak rate of each detector is measured below 2×10^{-3} l/hr. Pins, serving both as fixation points and for alignment, are inserted and glued on both ends of each carbon tube. A geometrical survey was performed and the measured radii are within 1 to 2 mm of the design values. Figure 5 shows a photograph of the curved BMT detectors.

As pointed out above, the BMT is located inside the CLAS12 5 T solenoid. The high magnetic field had a strong impact on the design and operation of the BMT detectors. Since the (detector) electric and the (solenoid) magnetic fields are essentially orthogonal, the primary electrons in the drift region of the Micromegas detectors are subject to Lorentz forces. Consequently, the electron trajectories form an angle with respect to the electric field direction, the so-called Lorentz angle. Hence, the charge is spread over a large area and this directly impacts the position resolution. Early studies showed that large Lorentz effects could be partly compensated for by using a 5-6 kV/cm drift high voltage [12]. This increase of the drift field impacts the efficiency through a loss of transparency of about $\approx 5\%$. The effect is worse in the case of the Z-type detectors with their strips parallel to the B-field direction. Finally, the gas mixture of 90% argon + 10% isobutane offers a reasonable trade-off between a limited drift velocity to reduce the Lorentz force effects and a high number of electrons generated in the conversion gap. The Lorentz angle is estimated to be about 40° in the 5 kV/cm drift electric field at 5 T.

2.5. Forward Micromegas Tracker (FMT)

The Forward Micromegas Tracker, shown in Fig. 6, consists of six identical Micromegas resistive detectors in the forward region from 30 cm to 36 cm downstream of the target center. Each Micromegas detector is a 450 mm diameter disk with an active area of 1024 parallel readout strips (525 μm pitch). The angle between the strip orientation of two adjacent disks is 60°. The distance between the readout strips of two consecutive disks is 10.5 mm. Each disk consists of an assembly of two 0.2-mm-thick PCBs glued on a 2 mm Rohacell foam backing to form the readout plane and a 0.2 mm PCB for the drift plane glued on two cylindrical frames that define the gas volume (5 mm). The inner frame is made of PEEK and the outer frame of aluminum. Both define the chamber and are attached to the readout plane using stainless steel screws. High voltage connections and associated filter circuits are located on the disk edge diametrically opposed from one another. The signals are read out via 16 MEC8 connectors.

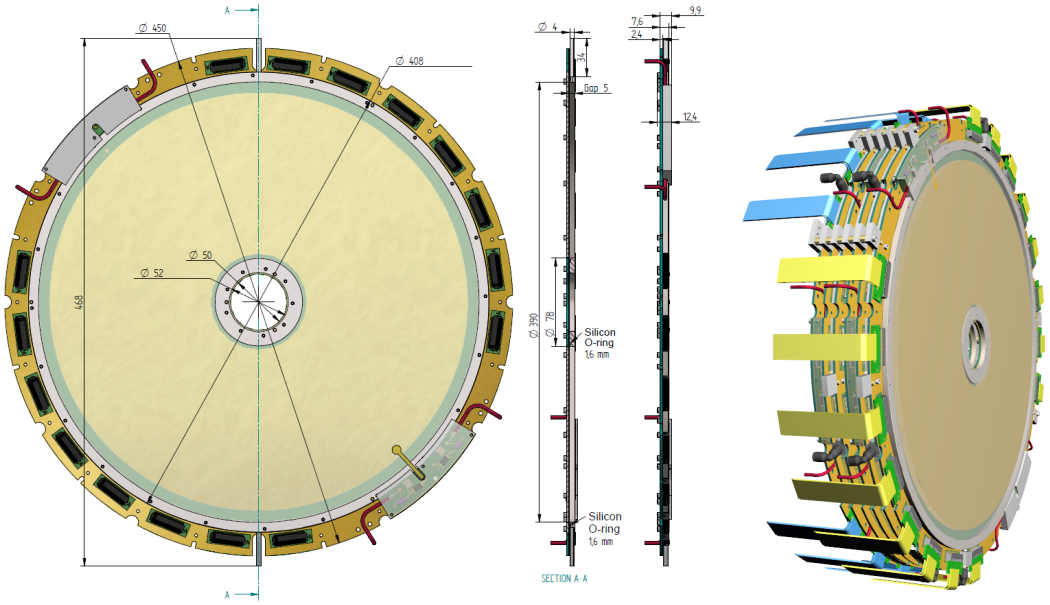

Figure 6: CAD views of the FMT disks.

The active area of the FMT is divided in two parts, the inner part with diameter $86 < d < 166$ mm and the outer part with $168 < d < 380$ mm. Each of the two parts can be independently energized so that the inner region can be turned off in the case of a very high flux of charged particles.

Since the magnetic field is parallel to the drift field in the FMT, the drift electrons are not affected by the Lorentz angle effect. In order to improve the timing resolution, a mixture of 80% argon + 10% isobutane + 10% CF_4 allows for an increase of the drift velocity compared to 90% argon + 10% isobutane mixture used in the BMT [13].

2.6. Gas System

The Micromegas are continuously flushed with gas in order to maintain high purity and to overcome the normal outgassing of the detectors. As stated above, the gas used for the BMT is a flammable mixture, argon with 10% isobutane. Each layer of the barrel is fed with one gas line. The tiles of a given layer are connected in series, with a flow rate of about 1.5 l/hr. For the FMT, the gas mixture is argon with 10% CF_4 and 10% isobutane with a flow rate of 2 l/hr for a set of three disks connected in series. Thus a total of ∼13 l/hr is used for both the FMT and BMT. Due to the low gas flow rate for the detectors, a gas recirculation system is not employed for the MVT.

A programmable logic controller controls the overall flow sent to the BMT and to the FMT, which is provided by a gas mixing system located outside of the experimental hall. As shown in Fig. 7 and Fig. 8, a gas control panel allows the gas distribution between the different lines for the BMT and FMT to be manually adjusted . Inside the gas control panel, the gas pressure and flow are measured at various points. The flow rate and pressure must be low and controlled to avoid any deformation of the detectors. Interlocks are set to close valves and stop the gas flow in the detector if pressures or flows are above the set thresholds. Finally, the total inflow and outflow are compared and trigger an interlock to stop the gas flow if they disagree, which could indicate a leak in the gas system or the detector volume.

3. Electronics

The MVT data acquisition system is designed to read out 6,000 channels of the forward station and 18,000 channels of the barrel station. With the physics background as high as 20 MHz, the strip hit rates are about 60 kHz and 20 kHz in the forward detectors and in the barrel detectors, respectively. The readout system is compliant with the CLAS12 requirements of a 20 kHz maximum trigger rate and provides a sufficiently long data pipeline to cope

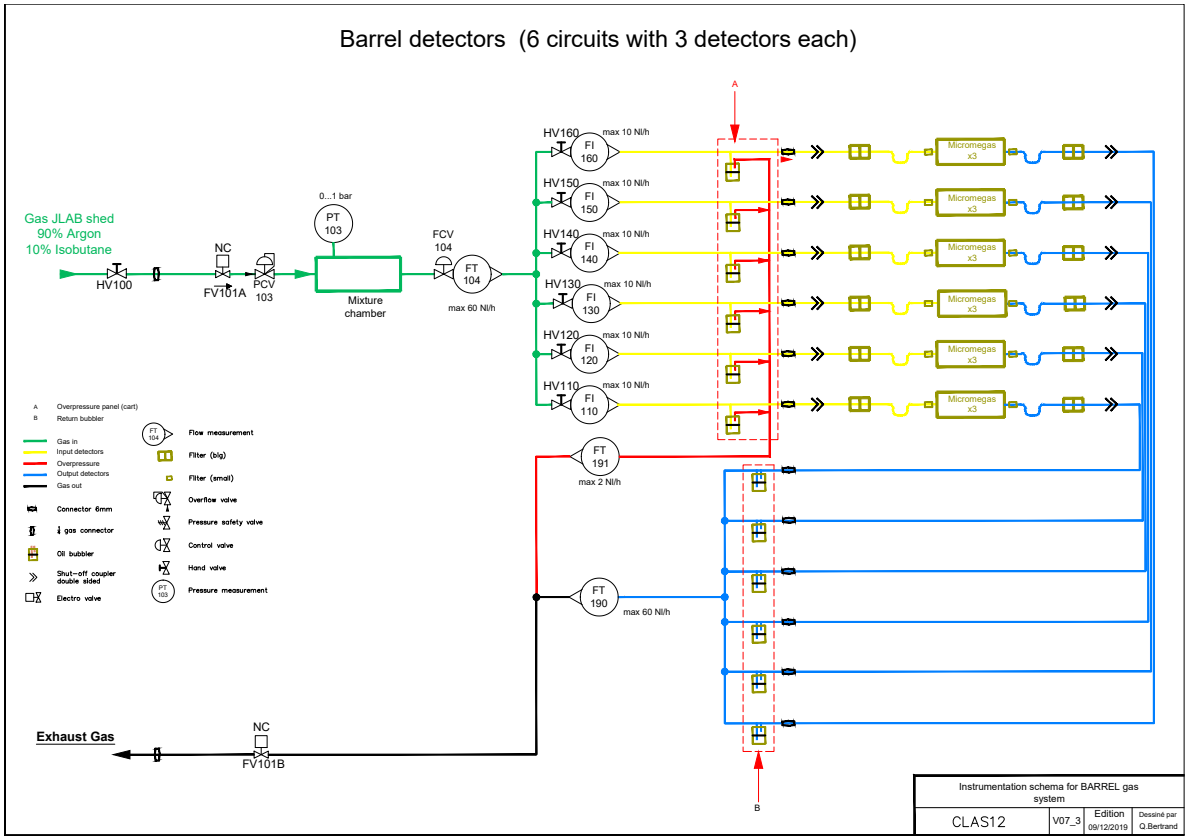

Figure 7: Gas distribution diagram for the Barrel Micromegas Tracker.

with up to a 16 μs trigger decision latency. Timing precision of a few ns is sufficient to limit the number of ghost hits compatible with the timing of the trigger signals. A charge measurement with a 10-bit dynamic range is enough to cover the full span of the Micromegas detector signals and to discriminate accurately minimum-ionizing particles (MIPs) from noise. Note that the FT-Trk [11] uses the same readout electronics and architecture as the MVT.

3.1. Readout System Architecture

The extremely compact and dense design of the CLAS12 Central Detector leaves a very narrow space between the MVT and its neighbor subsystems, as well as between the Micromegas detectors themselves. In addition to the stringent space limitations, the operational conditions of the tracker are harsh in terms of radiation and the high 5 T magnetic field. Keeping a low material budget is an obvious concern. Consequently, a readout architecture based on off-detector front-end electronics has been adopted. Lightweight micro-coaxial cable assemblies with low 40 pF/m linear capacitance carry bare, unamplified signals to the Front-End Units (FEUs) housed in crates ∼1.5–2 m upstream of the detectors.

The front-end electronics are responsible for the amplification and shaping of the detector signals, for holding the latter in a pipeline waiting for a trigger signal, for the digitization and compression of the selected event data, and for their delivery to the back-end electronics. The back-end is responsible for data concentration event by event. It provides an interface with the CLAS12 event building system, ensures a fixed latency path between the CLAS12 Trigger system [14] and the FEUs, and receives the system clock and trigger from the CLAS12 Trigger Supervisor and synchronously conveys them to the FEUs over bidirectional optical links. A schematic representation of the readout system architecture is shown in Fig. 9.

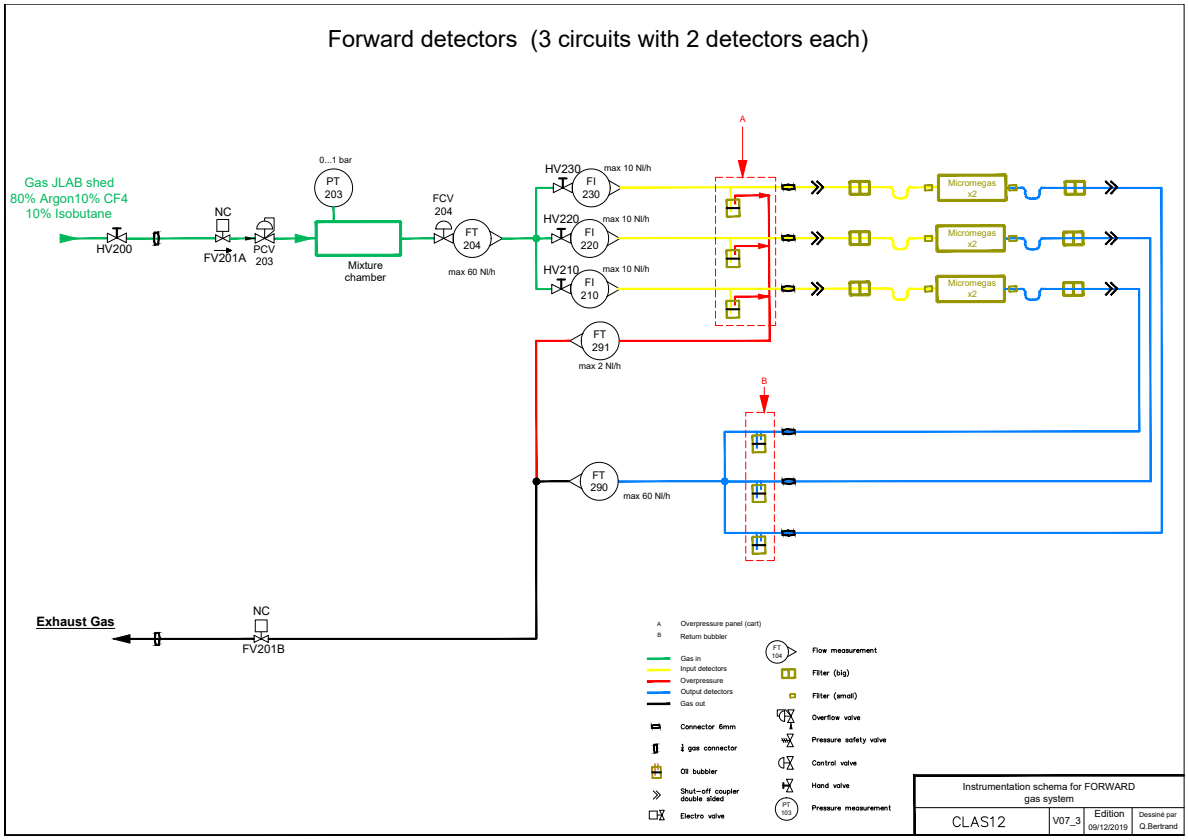

Figure 8: Gas distribution diagram for the Forward Micromegas Tracker.

3.2. The 64-Channel DREAM ASIC

Depending on the type and size of the CLAS12 Micromegas detectors, the strip capacitances vary from 60 to 120 pF. The total capacitance seen by the front-end electronics input is even higher, up to 200 pF due to the contribution from the detector micro-coaxial cables. To achieve a comfortable signal-to-noise ratio (SNR) well above 10, the equivalent noise charge (ENC) of the detection chain should be $\sim 2500\ e^-$ for the $140 - 200$ pF range of the total input capacitance. At the time of the detector development, no existing ASICs could deliver the required performance while, in addition, sustain the 20 kHz readout rate and provide the 16 μs deep trigger pipeline required. A new 64-channel ASIC, called DREAM (for Dead-timeless Readout Electronics ASIC for Micromegas), has been developed [15].

The DREAM ASIC block diagram is shown in Fig. 10. Each channel includes a charge sensitive amplifier (CSA) adapted to a wide spread of detector capacitances (up to 1 nF) and four selectable charge measurement ranges (from 50 to 600 fC), a shaper with programmable peaking times (from 75 ns to 1 μs), and 512-cell deep Switched Capacitor Array (SCA) used as the trigger pipeline memory and a de-randomization buffer.

The input signals are continuously sampled and stored in the SCA at a rate of up to 50 MHz. Upon reception of the trigger signal, a programmable number of samples of all channels, corresponding in time to the event, is read out serially through a differential analog buffer capable of driving an external ADC at a frequency of up to 28 MHz. The sampling is not stopped during the readout process, which allows nearly dead-timeless operation. Other features, such as the ability to operate with both signal polarities, the possibility to inject input signals directly into the SCA memory bypassing the filter and/or CSA, and integrated per-channel discriminators (useful to form trigger primitives), make the chip extremely versatile. The integrated circuit is manufactured in the AMS CMOS 0.35 μm technology and is encapsulated in the 128-

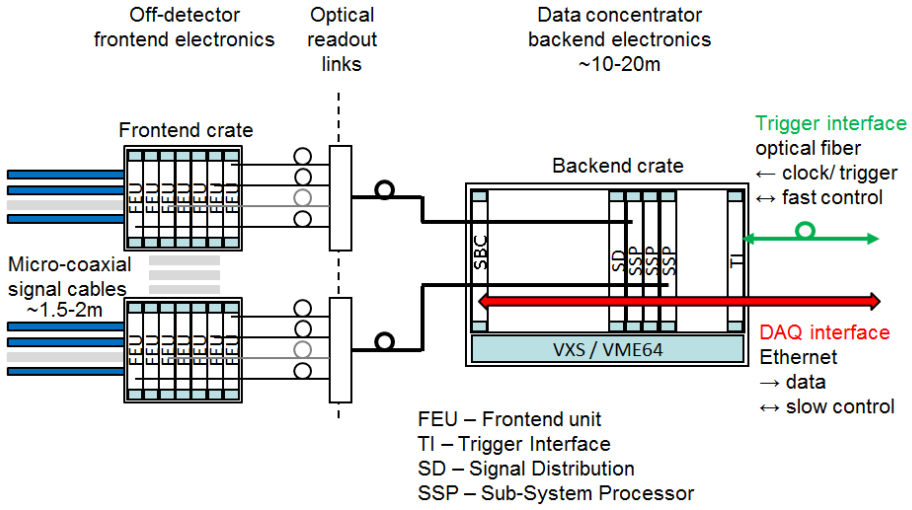

Figure 9: Readout system for the MVT and FT-Trk detectors.

pin LQFP square package with a 1 mm side and a 0.4 mm pitch.

3.3. The 512-Channel Front-End Unit (FEU)

The FEU is a mixed analog-digital electronics board. The analog section comprises eight input connectors, protection circuits, DREAM ASICs, and an 8-channel flash ADC (see Fig. 11). The protection circuits are optional. They are installed on the FEUs to protect the DREAMs from the sparks of standard Micromegas detectors. When working with resistive detectors, the input channels of the DREAM ASICs can be directly connected to the detector strips, improving the signal-to-noise ratio. The protected or non-protected type of FEUs are determined during their manufacturing.

As described above, the pre-amplification, shaping, and trigger pipeline functionalities are implemented in the DREAM chips. The analog samples from the eight DREAMs are digitized by an 8-channel 40 MHz 12-bit flash ADC AD9222 from Analog Devices [16]. The eight serial streams of digital data are delivered to the on-board FPGA. The digital section of the board comprises an xc6vlx75t-2-ff748 FPGA from the Xilinx Virtex-6 device family [17], its configuration memory, a 2 Mbyte synchronous SRAM, small form-factor pluggable (SFP) transceivers, an on-board clock synthesizer, and an auxiliary trigger interface circuit.

The FPGA controls the DREAM integrated circuits and the ADC, producing the sampling and readout clocks, as well as various required control signals. One of the SFP cages is populated with an optical transceiver module that is used to establish a synchronous communication channel with the back-end electronics over a 2.5 Gbit/s link. In the downstream direction, the link encodes the 125 MHz system clock, trigger signals, and fast synchronous commands.

Upon accepting the trigger signal, the FPGA reads the corresponding samples from the DREAMs and optionally applies the following digital data processing steps. First, after serial-to-parallel conversion, the pedestals are equalized. Next, for each sample, the coherent noise affecting the DREAM inputs is estimated and subtracted on a chip-by-chip basis. This greatly improves the noise immunity of the MVT readout system. Finally, the per-channel zero suppression is performed. The retained samples describe the signal development in the channel. Fitting their values with a known function allows an accurate estimation of the deposited charge and the signal timing. For each accepted trigger, the FPGA forms an event fragment from the retained channel data and delivers it to the back-end electronics via the optical channel. The optical channel is also used for setting and monitoring the run control parameters.

The FEU is a 6U (266 mm) high, 220 mm deep, and 5HP (25.4 mm) wide module. The thickness of its 12-layer PCB is 1.6 mm. It can be powered from either a 4.3 V or 5 V source and consumes slightly

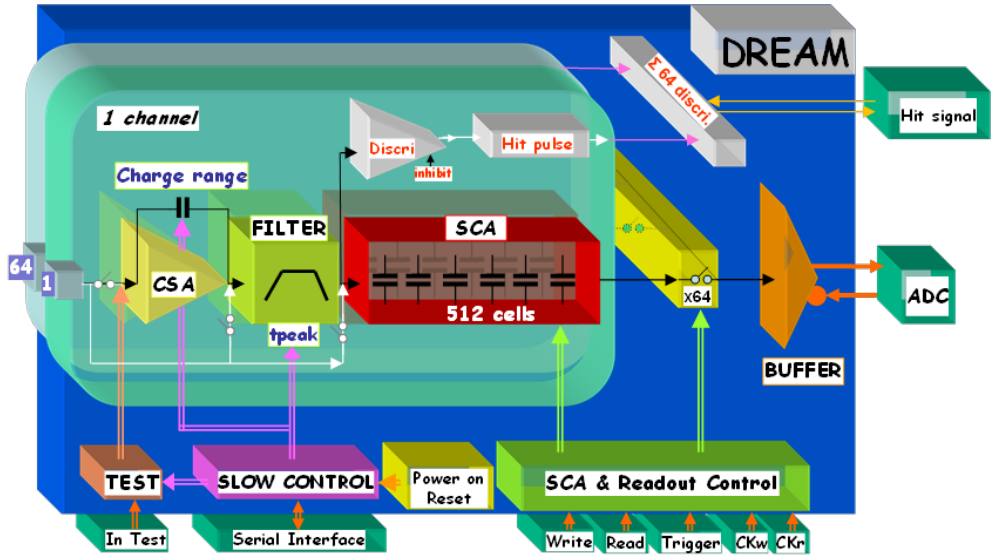

Figure 10: Block diagram of the DREAM ASIC.

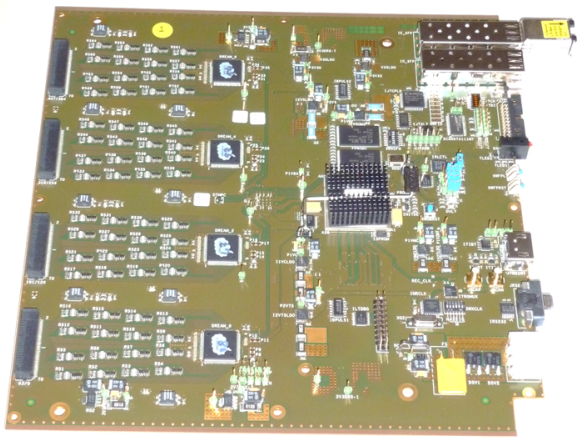

Figure 11: Photograph of the 512-channel Front-End Unit.

less than 20 W when all eight DREAMs operate in their most power-hungry mode. The FEUs have been operated in a magnetic field of up to 1.5 T without any perceptible change of their power consumption or functionality.

3.4. The Back-End Unit (BEU)

The back-end of the data acquisition system of the MVT is based on the JLab standard VME/VXS hardware including a Trigger Interface (TI), a Signal Distribution (SD), a Subsystem Processor (SSP), and a crate controller single-board computer (SBC) [18]. The flow of the trigger, data, and control messages is shown in Fig. 9.

The TI receives a low-jitter, 250 MHz system clock and fixed-latency trigger signals from the CLAS12 Trigger Supervisor. It also delivers to the Trigger Supervisor the status information (e.g. busy) of the MVT readout system. The physical layer interface is based on parallel optic technology. The clock and trigger signals are delivered to the SD board over the VXS backplane. The SD board conveys properly delayed and aligned clock and trigger signals to the SSP boards. It also gathers their status information, and then combines and sends it to the TI board. These communications happen over the VXS backplane.

The SSP board was primarily designed to be a part of the hardware-level trigger logic for JLab experiments. Given the massive resources it provides (notably a Virtex-5 TX150T Xilinx FPGA, 32 multi-gigabit transceivers (GTX) routed to the front panel, 4 Gbyte DDR2 memory), it was considered for the readout of the MVT front-end electronics. The SSP firmware has been modified to fit the needs of the MVT Back-End Unit (BEU).

An SSP can distribute the global system clock, trigger, and synchronous commands to up to 32 FEUs. In practice, there are two Back-End Units each serving 24 front-ends. The trigger pulses and fast run control commands are broadcast synchronously to all FEUs over the synchronized fixed latency 2.5 Gbit/s links. The protocol between

the FEUs and the BEU sets an 8 ns resolution on successive triggers and synchronous commands (125 MHz clock). However, the dispersion of their arrival times on the FEUs is well under 1 ns.

On each trigger, the SSPs time stamp the event with the synchronous 125 MHz clock and assign it the event counter value. The 48-bit time stamp along with the 60-bit event identification (ID) is used for local event building. This process implies gathering from all FEUs the event data packets belonging to the same event (matching time stamps, and event IDs). Multi-event buffers, with a programmable number of events, are constructed in the external DDR2 memory. Upon the request from the crate controller SBC, the contents of the buffers are transferred to its memory over the VME64 backplane using the 2SST protocol. Transmission rates of ∼200 Mbyte/s are routinely achieved.

The SBC executes the data collection and the run control tasks within the CODA software framework [18]. It also completes the data integrity checks performed in the SSP firmware, disentangles multi-event buffers, forms MVT events concatenating the FEU/SSP data with the corresponding TI data, and sends them to the CLAS12 Event Builder over a 10 GB/s Ethernet link.

The MVT readout electronics is continuously monitored by the CLAS12 detector monitoring system using the EPICS framework.

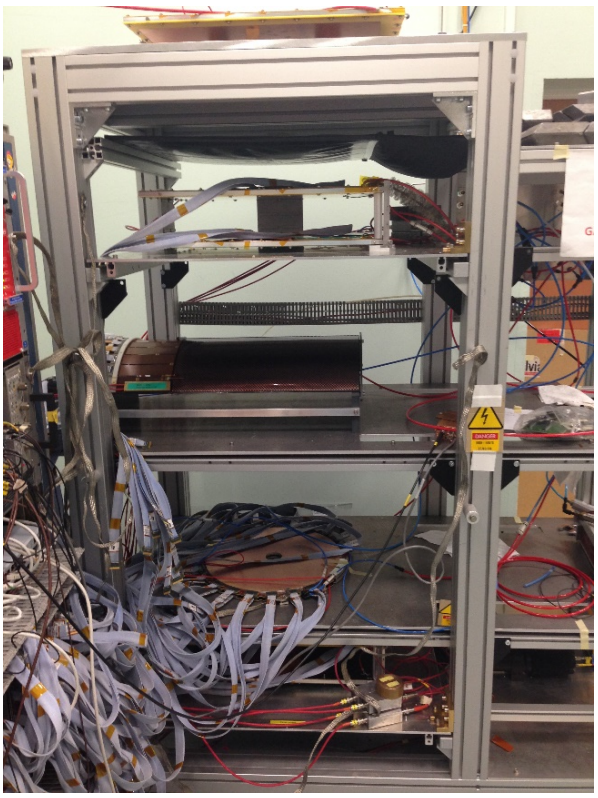

Figure 12: The cosmic bench made of an external trigger from the coincidence of two scintillators and a hodoscope made of 4 reference trackers. The photograph shows the simultaneous operation of a BMT tile and a FMT disk under test.

4. Detector Performance

In order to calibrate the detectors and test their performance, a cosmic-ray test bench was designed and installed at Saclay early in the project. The goal of these tests was to determine the best operating conditions of the detectors and to compute their 2D efficiency maps using cosmic muons prior to their shipment to JLab.

The cosmic-ray test bench shown in Fig. 12 consists of a vertical stack of six detectors. Two scintillators are installed at the top and the bottom of the stack to provide the trigger. Four 50×50 cm^2 double-layer flat Micromegas were used as a tracker to provide the reference track of a cosmic ray. In the middle of the stack, empty trays receive the detectors to be characterized.

After alignment of the reference trackers and the detectors to be tested, the expected position of the particle in the test detector was provided by the reference trackers and compared with the measured signals, if any, in the test detector. If a cluster, i.e. a contiguous set of fired strips, matched the expected position within a millimeter, the test detector was considered to have seen the cosmic ray. The efficiency was then derived by repeating this test over a cosmic ray sample collected within a few hours. All MVT detectors were systematically characterized before shipment to JLab. These tests included a study of the efficiency as a function of the amplification voltage and a two-dimensional efficiency map, which required a cosmic ray sample collected over a day.

The results were found to be similar for all detectors. The efficiency plateau starts at about 500 V with a value between 98.5% and 99.5% at 510 V. It was shown that the plateau was slightly shifted to higher strip voltages when the drift plane was at higher voltage because the mesh loses electron transparency. The 2D-efficiency map was useful to look for any structural problems. All MVT

detectors that were shipped to JLab had a uniform 2D-efficiency map. Examples of the efficiency plateau and the 2D efficiency map are shown in Figs. 13 and 14. Figure 14 also shows the efficiency gained by removing the protection diodes before the Dream ASICs, not required with resistive Micromegas since sparks are quenched.

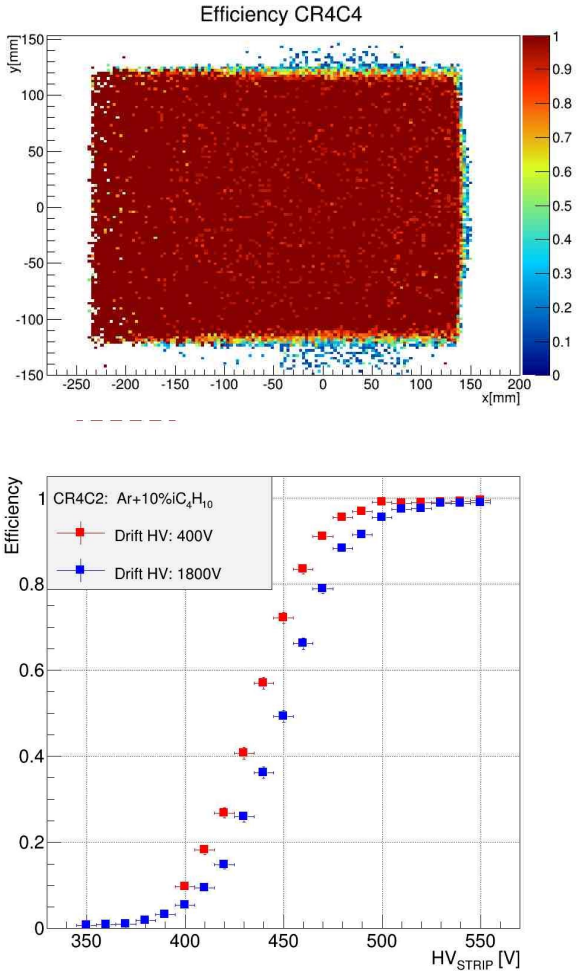

Figure 13: Efficiency plateau (bottom) and 2D efficiency map (top) for a C-type barrel detector.

4.1. Commissioning

The Micromegas Vertex Tracker was delivered to JLab in June 2017. A team of 10 people assembled the MVT and integrated it with the SVT to form the final configuration of the CLAS12 Central Vertex Tracker. The MVT barrel was first commissioned with cosmic rays in the assembly room until mid-October 2017 and for the first two weeks

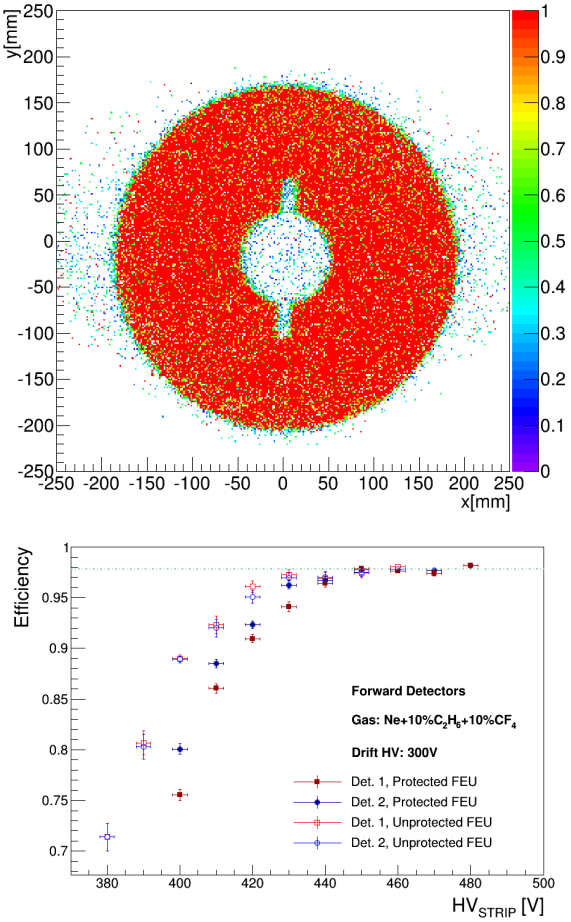

Figure 14: Efficiency plateau (bottom) and 2D efficiency map (top) for a FMT disk.

after it was installed in Hall B. The final phase of the commissioning started in December 2017 with beam.

Before the start of data taking with beam, several cosmic ray runs were performed aimed at tuning and optimizing the integration of the data acquisition system and the slow controls (i.e. remote controls, interlocks, and monitoring) [18], and the gas delivery system. The online data monitoring system was developed to allow the inspection of raw quantities such as the hit maps, the pulse shape, and the timing of the signals. This system was tested and integrated into the standard CLAS12 online operation tools.

4.2. Cosmic Ray Data Taking

Cosmic ray data with zero magnetic field were used not only for commissioning purposes, but also

for the essential detector alignment. Given the absence of the solenoid magnetic field, the drift high voltages were set to about 400 V as the primary electrons do not experience the Lorentz-angle effect. The cosmic ray trigger for the Central Detector was provided by coincidences of CTOF signals in diametrically opposed scintillator bars. This CTOF trigger provides a quasi-uniform illumination along the BMT axis of the barrel with cosmic rays, not achievable in beam conditions because of the forward-peaked distribution due to the center-of-mass boost. The hit distribution on the Z tiles, instead, results from a convolution of the cosmic ray angular distribution with the trigger configuration, as shown in Fig. 15.

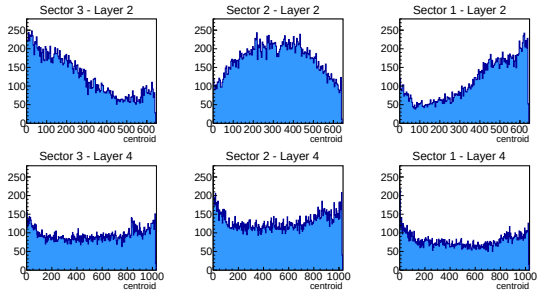

Figure 15: Hit occupancies of a cosmic-ray run with the trigger delivered by the CTOF for layers 2 (Z tile) and 4 (C tile).

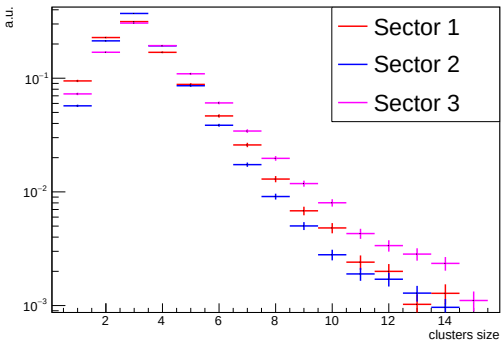

Figure 16: Cluster size distributions, i.e. the number of strips fired in a tile by a cosmic ray, during cosmic ray data taking for the three sectors of the Z tiles.

The distributions of cluster size for the three sectors (see Fig. 16) show, on average, larger clusters in Sectors 1 and 3 with respect to Sector 2. Indeed, since cosmic rays are mostly vertical, the projection of their path in the drift gap onto the strip surface is longer for Sectors 1 and 3 than for Sector 2.

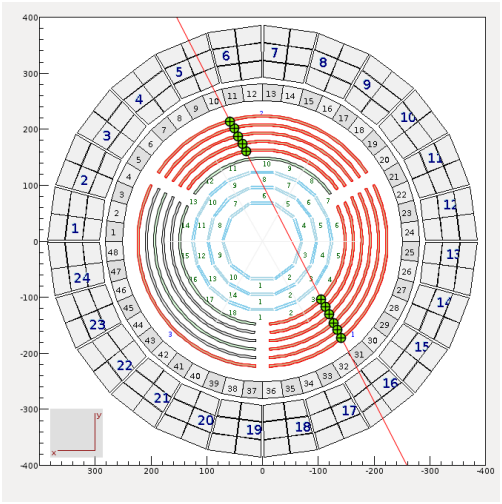

Figure 17: Event display of a cosmic ray track reconstructed in the BMT detectors. The six tiles on the top are called Sector 2, the six on the bottom right are Sector 1 and the bottom left six tiles are the Sector 3.

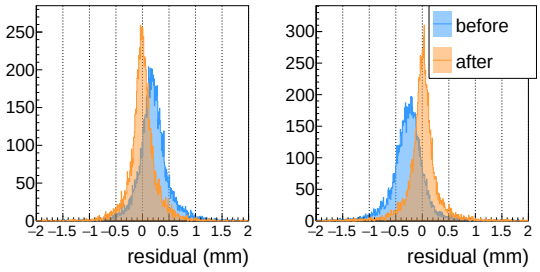

Figure 18: Example of residuals for two BMT tiles with cosmic ray data before and after a preliminary alignment procedure obtained with a BMT stand-alone reconstruction.

A BMT stand-alone straight-track reconstruction algorithm based on least-squares minimization has been developed to reconstruct cosmic rays. A typical reconstructed event is shown in Fig. 17 using the CLAS12 event display package [19]. This tracking algorithm is also used to perform the alignment of the BMT tiles: the distance between the hit in a tile excluded from the tracking and the reference track provided by the other tiles is minimized by introducing rotations and translations. Figure 18 shows the distributions of track residuals, i.e. the distance of a hit with respect to the particle trajectory, for three Micromegas tiles before and after alignment corrections. Figure 19 shows the summary of the preliminary results for all BMT de-

tectors: after the alignment procedure all residual distributions are centered around zero. Preliminary detector resolutions, defined as the standard deviations of Gaussian fits to the residual distributions, are improved and below 200 μm.

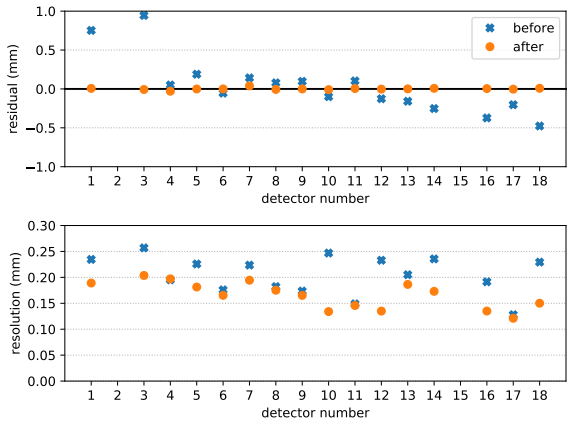

Figure 19: Preliminary BMT residuals (top) and resolutions (bottom) with cosmic-ray data before and after an alignment procedure obtained with a BMT stand-alone reconstruction.

4.3. Data Taking with Beam

With the start of beam operations, the behavior of the detectors has been carefully monitored and the working parameters such as high voltage settings have been tuned. The working point for the strip high voltage has been studied by performing a scan with a 20 V step. Due to delays in the offline data reconstruction for a proper efficiency measurement, the cluster multiplicity per electron trigger was used as an alternative observable accessible online that can be used to exhibit a plateau. Indeed, as shown in Fig. 20, this observable was found to flatten out where the efficiency plateau was determined from the commissioning with cosmic rays. For the FMT, the plateau was found from 460 V to 490 V. Above 490 V, the cluster multiplicity and the current on the strips increases suddenly, potentially due to a Corona effect. It was decided to set 460 V as the nominal HV settings for the FMT, which allows safe operations for luminosities up to 10^{35} cm^{-2}s^{-1}. The nominal HV setting was set to be 520 V for the BMT, although the plateau was not as clear as for the FMT.

Preliminary efficiencies for the Micromegas detectors were measured by performing tracking without the detector layer under study to determine for

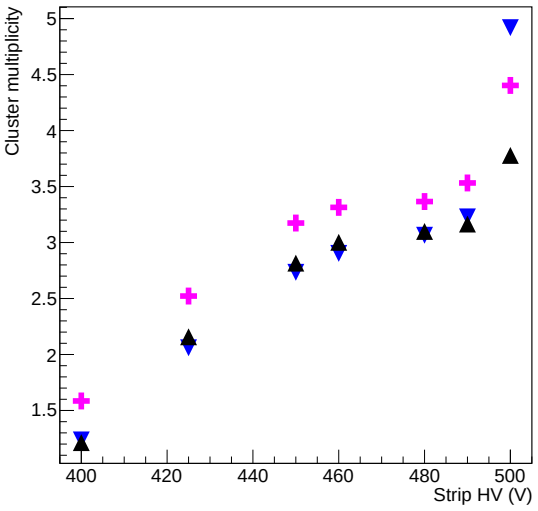

Figure 20: Cluster multiplicity in 3 FMT disks as a function of HV on the strips.

each track going through the studied detector layer, if a hit was found close to the expected intersection. The efficiency plateau was found to be at the same position as the plateau with the cluster multiplicities, thus validating the HV settings used. An example of the efficiency scan for one BMT tile is shown in Fig. 21.

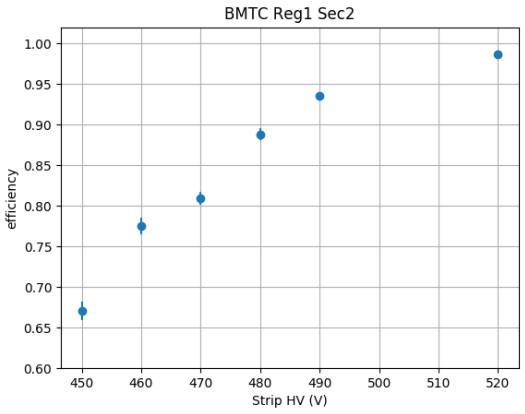

Figure 21: Efficiency measurement as a function of the strip high voltage for one BMT tile in beam conditions.

Strip currents and detector occupancy have been measured during a beam intensity scan up to the instantaneous luminosity of about 10^{35} cm^{-2}s^{-1}. Figure 22 shows the correlation between the cur-

rents drawn by the BMT strips and the beam current. The slope coefficient resulting from a linear regression is 0.02 μA/nA. At the maximum beam current of 78 nA, two BMT tiles reached the safety threshold of 2 μA and they were automatically turned off. The detector occupancy shows as well a linear correlation with the beam current, reaching values of about 3.5% for the FMT disks and 2.5% for the BMT tiles at nominal luminosity, as shown in Fig. 23.

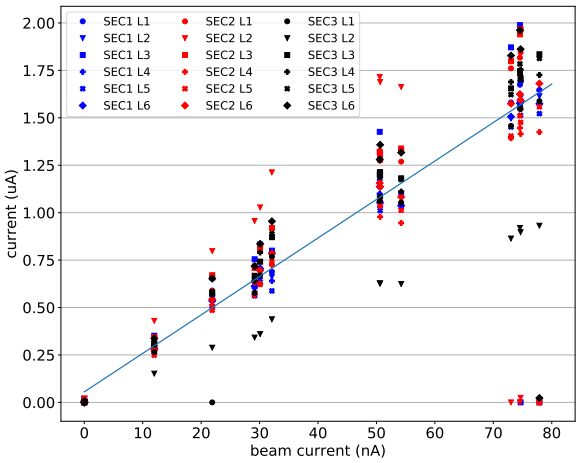

Figure 22: Currents on the BMT strips as a function of beam current on a 5-cm-long liquid-hydrogen target. All detectors have similar currents. The nominal luminosity of 10^{35} cm^{-2}s^{-1} corresponds to 75 nA on target.

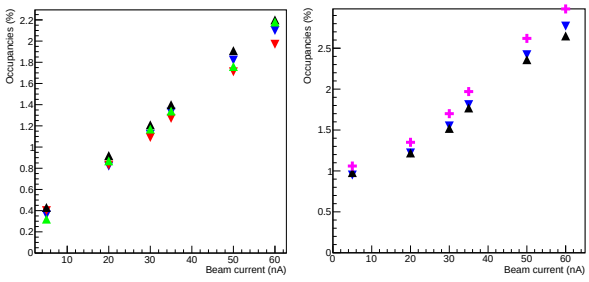

Figure 23: Hit occupancy as a function of the beam current for 4 BMT layers (left) and 3 FMT disks (right).

During the first year of operations with beam, CLAS12 took data at several electron beam energies (2.2, 6.4, 7.5, and 10.6 GeV) with a liquid-hydrogen target. An example of a rare event at 10.6 GeV with five tracks reconstructed in the CVT is shown in Fig. 24. At 2.2 GeV, the large elastic cross section and the trigger configuration allowed for the visualization of the recoil protons in the raw occupancies of the BMT-C tiles as seen in Fig. 25.

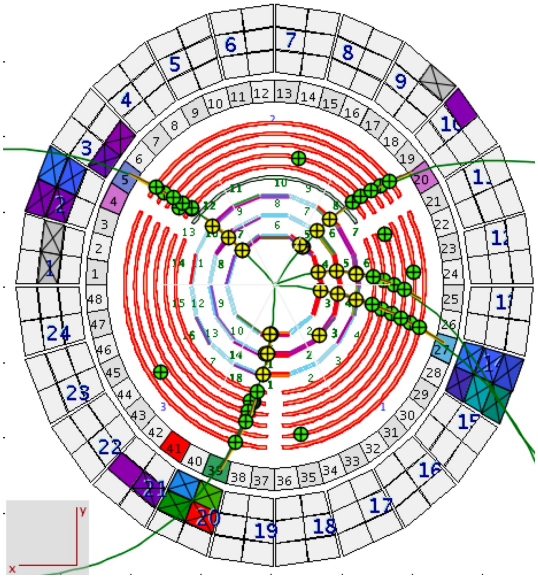

Figure 24: Event display of a rare five-track event in the CVT.

The largest data set has been collected at an electron beam energy of 10.6 GeV and at 50 nA intensity. Figure 26 shows the distributions of the number of clusters on all six BMT layers and their cluster size distribution. Although most of the events present a very low number of clusters with clusters of small size, the long tails are mainly due to knock-off electron "loopers" and beam-induced soft photons.

Each MVT hit has an associated time stamp that can be used to compute the time difference of the signal with respect to the trigger. Consequently, a minimum time T_{min} can be associated with each cluster as the minimum time of the hits in the cluster. Figure 27 clearly shows that the clusters that have been associated with a reconstructed track have similar T_{min} distributions over the six BMT layers, i.e. the clusters associated with a triggered physics event are strongly correlated in time. However, the T_{min} distributions of background clusters, i.e. clusters that are not associated with reconstructed tracks, are uniform in time except for very low T_{min} values. The excess of events at low T_{min} for all layers is explained by the asymmetric shape of the pulse: since the tail of the pulse is much longer than the leading edge of the pulse, it is more likely to get out-of-time clusters prior to than after the trigger.

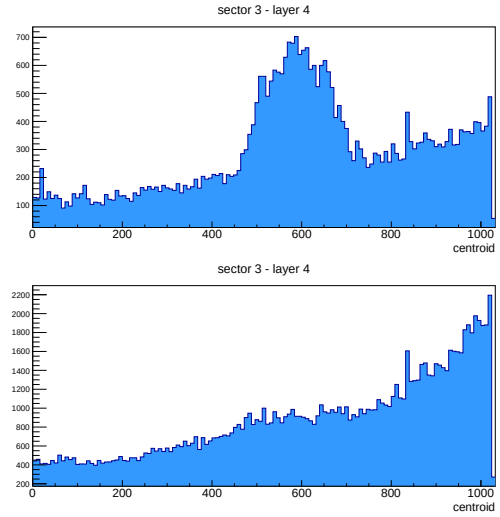

Figure 25: Hit occupancy for C tiles at 2.2 GeV (top) and 10.6 GeV (bottom) in events triggered by an electron in the forward CLAS12 detectors. The elastic recoil protons are responsible for the large excess of events at 2.2 GeV between strip number 400 and 700. At 10.6 GeV, the elastic cross section is too small and no clear proton excess is visible.

Special data taking runs with an empty target cell have been performed for calibration purposes, as well as low-luminosity runs with zero magnetic field for detector alignment studies. The stand-alone straight-track algorithm used for cosmic ray reconstruction has been adapted and extended to use SVT hits. Using preliminary alignment corrections for both the SVT and BMT, a zero-field empty-target run was reconstructed in SVT-stand-alone mode and CVT (i.e. SVT+BMT) mode. The preliminary results are shown in Fig. 28. The aluminum target walls are clearly visible in both reconstruction modes. There is a significant improvement from ∼4.5 mm to 2.5 mm of the vertex position resolution (1σ) along the beam axis when the BMT information is used in the track reconstruction. Indeed the BMT-C tiles largely improve the polar angle of the particle with respect to the SVT-stand-alone mode. Concerning the azimuthal angle, the resolution of the BMT-Z tiles is not as good as that of the SVT modules since the strip pitch is larger and they are further away from the beam axis. Therefore the improvement of the resolution on the azimuthal angle of the track and related quantities like the vertex transverse coordinates is limited. On the other hand, the BMT-Z tiles provide an essential redundancy for tracks that cross a limited number of SVT layers.

5. Conclusions

In this paper, the CLAS12 Micromegas Vertex Tracker system is presented. The mechanical structure of the Forward and the Barrel Micromegas Trackers, the first curved detector of this size using the Micromegas technology, is described. The architecture and performance of the readout electronics are presented, including the DREAM ASIC, developed to achieve the performance required by the CLAS12 specifications. The Micromegas Vertex Tracker performance with cosmic rays is shown, as well as some preliminary results with beam data to demonstrate a significant improvement in the reconstruction in the central tracker.

6. Acknowledgements

We are grateful to D. Abbott, S. Boiarinov, C. Cuevas, J. W. Gu, B. Moffit and A. Stepanyan from JLab for their continuous help at various phases of the project. We would like to thank the Hall B staff, the JLab Detector Support Group, and Y. Gotra for their support on the MVT project.

This material is based upon work supported by the U.S. Department of Energy, Office of Science, Office of Nuclear Physics under contract DE-AC05-06OR23177. This research was funded in part by the French Agence Nationale de la Recherche contract no.37.

[1] V. D. Burkert, et al., The CLAS12 Spectrometer at Jefferson Laboratory, to be published in Nucl. Inst. and Meth. A, (2020) (see this issue).

[2] M. A. Antonioli, et al., The CLAS12 Silicon Vertex Tracker, to be published in Nucl. Inst. and Meth. A, (2020) (see this issue).

[3] M. D. Mestayer, The CLAS12 Drift Chamber System, to be published in Nucl. Inst. and Meth. A, (2020) (see this issue).

[4] S. Procureur, Simulation of Micromegas Detectors for the CLAS12 Central Tracker, CLAS-Note 2007-004 (2007).

[5] S. Aune, *et al.*, Simulation of Micromegas Detectors for the CLAS12 Central Tracker, CLAS-Note 2010-003 (2010).

[6] D. S. Carman, et al., The CLAS12 Central Time-of-Flight System, to be published in Nucl. Inst. and Meth. A, (2020) (see this issue).

[7] P. Chatagnon, et al., The CLAS12 Central Neutron Detector, to be published in Nucl. Inst. and Meth. A, (2020) (see this issue).

[8] Y. Giomataris, P. Rebourgeard, J. Robert, G. Charpak, Micromegas: A high-granularity position-sensitive gaseous detector for high particle-flux environments, Nuclear Instruments and Methods in Physics Research Section A: Accelerators, Spectrometers, Detectors and Associated Equipment 376 (1) (1996) 29 – 35.

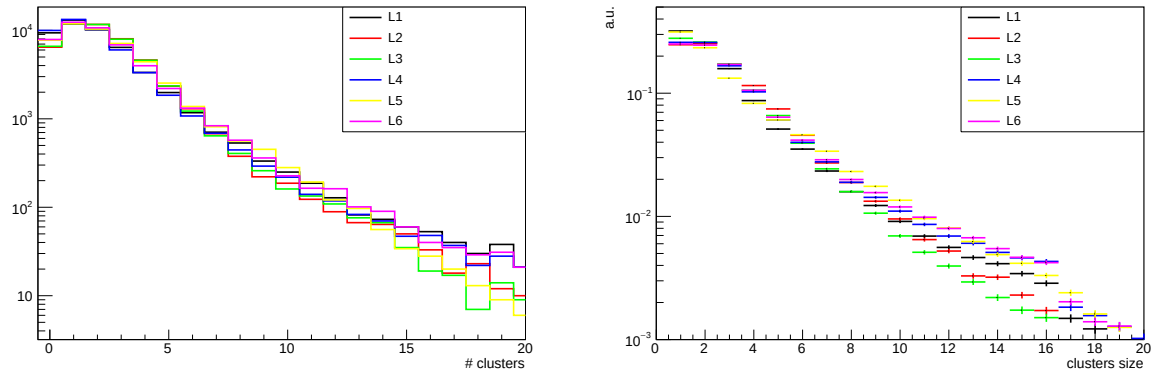

Figure 26: (left) Number of clusters per event and (right) cluster size distribution in the BMT layers. The beam current was 50 nA.

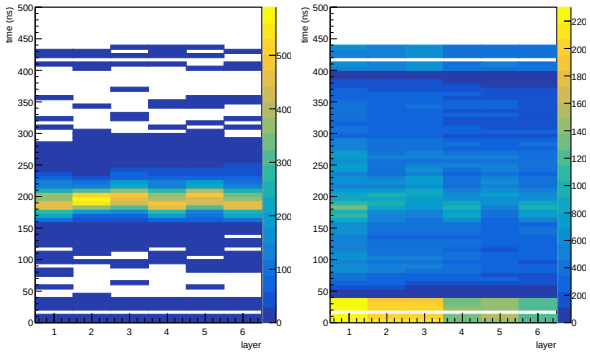

Figure 27: (left) Time distribution in the six BMT layers for clusters associated with a track; (right) Time distribution for clusters not associated with a reconstructed track.

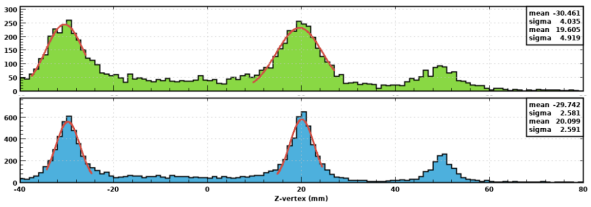

Figure 28: Preliminary vertex position along the beam axis reconstructed with the SVT-stand-alone reconstruction (top-green distribution) and the CVT reconstruction (bottom-blue distribution) for an empty-target and no solenoid field. The target walls are located at -30 and 20 mm with gaseous hydrogen in-between. At 50 mm, the scattering chamber endcap is clearly visible. The improvement in the resolution from the SVT to the CVT reconstruction is mainly due to the BMT-C tiles.

URL http://www.sciencedirect.com/science/article/pii/0168900296001751

[9] T. Alexopoulos, J. Burnens, R. de Oliveira, G. Glonti, O. Pizzirusso, V. Polychronakos, G. Sekhniaidze, G. Tsipolitis, J. Wotschack, A spark-resistant bulk-micromegas chamber for high-rate applications, Nuclear Instruments and Methods in Physics Research Section A: Accelerators, Spectrometers, Detectors and Associated Equipment 640 (1) (2011) 110 – 118. doi:https://doi.org/10.1016/j.nima.2011.03.025.
URL http://www.sciencedirect.com/science/article/pii/S0168900211005869

[10] I. Giomataris, R. D. Oliveira, S. Andriamonje, S. Aune, G. Charpak, P. Colas, G. Fanourakis, E. Ferrer, A. Giganon, P. Rebourgeard, P. Salin, Micromegas in a bulk, Nuclear Instruments and Methods in Physics Research Section A: Accelerators, Spectrometers, Detectors and Associated Equipment 560 (2) (2006) 405 – 408. doi:https://doi.org/10.1016/j.nima.2005.12.222.
URL http://www.sciencedirect.com/science/article/pii/S0168900205026501

[11] M. Battaglieri, et al., The CLAS12 Forward Tagger, to be published in Nucl. Inst. and Meth. A, (2020) (see this issue).

[12] P. Konczykowski, S. Aune, J. Ball, M. E. Yakoubi, C. Lahonde-Hamdoun, O. Meunier, S. Procureur, F. Sabati, S. Cazaux, E. Delagnes, S. Lhenoret, A. Mohamed, Measurements of the lorentz angle with a micromegas detector in high transverse magnetic fields, Nuclear Instruments and Methods in Physics Research Section A: Accelerators, Spectrometers, Detectors and Associated Equipment 612 (2) (2010) 274 – 277. doi:https://doi.org/10.1016/j.nima.2009.10.105.
URL http://www.sciencedirect.com/science/article/pii/S0168900209020567

[13] S. Procureur, Micromegas: A Tracking Detector for High Energy Physics and Beyond, habilitation à Diriger des Recherches, IRFU-15-73, 10 decembre 2015 (2015).

[14] B. Raydo, et al., The CLAS12 Trigger System, to be published in Nucl. Inst. and Meth. A, (2020) (see this issue).

[15] C. Flouzat, *et al.*, Dream: a 64-channel Front-end Chip with Analog Trigger Latency Buffer for the Micromegas

Tracker of the CLAS12 Experiment, TWEPP 2014 Topical Workshop on Electronics for Particle Physics, Centre des Congrès - Aix en Provence, France (22-26 September 2014).

[16] Analog Devices, AD9222: Octal, 12-Bit, 40/50/65 MSPS Serial LVDS 1.8 V A/D Converter, datasheet, Rev. D.

[17] Xilinx, Virtex-6 Family Overview, DS150, v2.4 (January 19, 2012).

[18] S. Boyarinov, et al., The CLAS12 Data Acquisition System, to be published in Nucl. Inst. and Meth. A, (2020) (see this issue).

[19] V. Ziegler, et al., CLAS12 Event Reconstruction, to be published in Nucl. Inst. and Meth. A, (2020) (see this issue).